QUANTUM MATERIALS

Plasmonic imaging is gaining momentum

Terahertz nanospectroscopy reveals many-body interactions in graphene

By **D. N. Basov**[1] *and* **M. M. Fogler**[2]

High-temperature superconductivity, unconventional magnetism, and charge-ordered states are examples of the spectacular properties that arise in solids through many-body effects, a consequence of electrons strongly interacting with one another and with the crystal lattice. In a seminal contribution, Landau introduced quasiparticles, objects that behave in many ways as free electrons but with velocities and masses altered or "renormalized." Information about the renormalization is encoded, for example, in optical properties of materials (*1*). The majority of optical studies have focused on response functions that depend on frequency ω, but dependence on momentum q, which is equally valuable, has remained beyond the reach of common spectroscopic tools. On page 187 of this issue, Lundeberg *et al.* (*2*) developed a means to probe the nonlocal or q-dependent electromagnetic response by harnessing surface plasmon polaritons (plasmons). Implications of the first results by Lundeberg *et al.* transcend the studies of graphene, their model system.

Plasmons can be regarded as coupled oscillations of electron density and electromagnetic field at frequency ω_0. Imaging of plasmonic waves in real space by scanning near-field optical microscopy is well suited for probing the response functions of two-dimensional (2D) materials, including graphene (*3*). However, investigation of many-body effects in graphene by Lundeberg *et al.* demanded that the plasmon imaging be done with low-frequency terahertz radiation. They accomplished this difficult task using a combination of near-field optics, scanned-probe imaging, and photocurrent measurements, as previously described by the same collaborative team (*4*). To study the plasmons, they fabricated structures in which graphene was separated from gold back gate electrodes by insulating boron-nitride spacers only a few nanometers in thickness.

The wavelength of plasmonic modes measured in these experiments was nearly 300 times smaller than the wavelength of terahertz photons. The corresponding plasmon momentum was nearly 300 times larger than the free-space photon momentum ω_0/c, where c is the speed of light. The reason for this large confinement factor is the proximity of graphene to the back gate, which screened Coulomb interactions and forced the plasmon velocity to approach the Fermi velocity v_F of graphene quasiparticles (see the figure). For these "slow" plasmons, the many-body renormalization of the plasmon dispersion is more apparent than in common graphene structures in which interactions are not screened.

Remarkably, the plasmon dispersion $\omega(q)$ determined by Lundeberg *et al.* is in accord with parameter-free theoretical calculations. These calculations link the renormalized plasmon dispersion to the "hourglass" shape of the electronic bands in graphene (see the figure, top), a salient product of many-body interactions (*5*). By taking into account additional dynamical correlations of the quasiparticles, the authors achieved a near-perfect agreement between the theory and their plasmonic imaging data.

Ramifications of many-body physics in graphene are demonstrably different from the behavior of other complex and synthetic conductors. Notably, the theoretical discussion of many-body physics in honeycomb carbon preceded the isolation of graphene by almost a decade (*6*). However, early measurements at the rise of graphene research seemed to suggest noninteracting Dirac quasiparticles (*7*). Among conspicuous exceptions were the hints of v_F enhancement at relatively low carrier density inferred from infrared spectroscopy (*8*).

The change in shape of the electron and hole bands from simple Dirac cones to an hourglass when interactions are present was firmly established by transport experiments with high-mobility samples (*5*). In contrast, electronic correlations in synthetic metals, such as transition metal oxides, induce "flattened" electronics bands (*1*), in contrast to graphene's hourglass-like renormalization. Likewise, plasmons in graphene acquire higher velocity because of many-body effects (*2*), unlike the response of correlated 2D synthetic conductors, in which interactions further slowdown plasmons (*9*). The physical reason for intricate differences of renormalization effect in graphene and other syn-

Electrons and plasmons in graphene

Lundeberg *et al.* used terahertz imaging of the surface of graphene near a gold film to determine plasmonic dispersion (their frequency ω versus momentum q, where the slope is their velocity v).

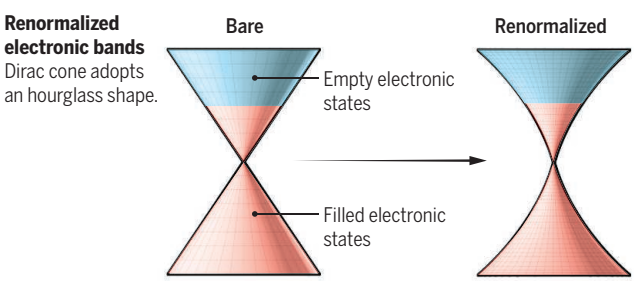

Renormalized plasmon dispersions
Slow plasmons (**3, 4**) are prone to renormalizations by many-body interactions. The net effect is enhanced plasmon velocity; **c** is the speed of light.

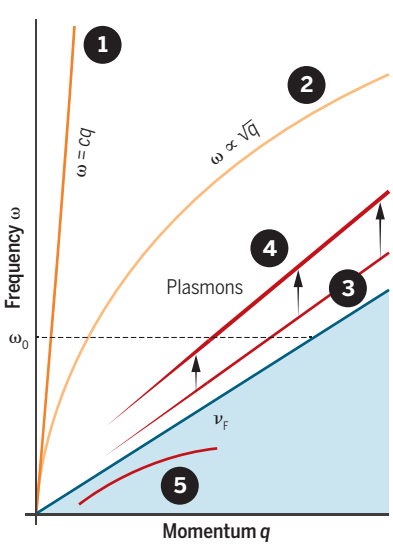

1 Photons in free space disperse as $\omega = cq$.

2 In free-standing graphene, plasmons disperse as $\omega \propto \sqrt{q}$ and their velocity is reduced compared to c.

3 Plasmons in graphene on gold become nearly as slow as the Fermi velocity v_F.

4 Many-body effects renormalize the velocity of "slow" plasmons.

5 "Demon" modes have yet to be seen.

[1]Department of Physics, Columbia University, New York, NY 10027, USA. [2]Department of Physics, University of California San Diego, La Jolla, CA 92093, USA. Email: db3056@columbia.edu; mfogler@ucsd.edu

GRAPHIC: C. BICKEL/*SCIENCE*

thetic conductors is the absence of a band gap in the former. Electrons can strongly interact with holes in gapless graphene (*6*), and this process changes the "sign" of the velocity renormalization correction compared with the case of electron-electron interaction.

Strong electron-hole interactions may cause the electronic liquid in graphene to become highly viscous (*10*). The mutual viscous friction forces electrons and holes to move together, so that the effective charge contributing to the low-frequency optical response of the electron liquid is diminished. In theory, this effect should inhibit plasmons but enable another type of collective excitation—energy waves or "demons" (*11*)—to exist at small ω and q (see the figure). The thermal photocurrent mapping technique devised by Lundeberg *et al.* (*2*, *4*) appears to be particularly promising for detection of these elusive modes.

Lundeberg *et al.* point out that their method of determining the nonlocal complex conductivity $\sigma'(\omega,q)+i\sigma''(\omega,q)$ is applicable to other quantum materials, including low-dimensional conductors, superconductors, and Weyl semimetals. A technical precondition for such experiments is the ability to use nano-optical imaging at cryogenic temperatures, which recently became available (*12*). Plasmonic imaging in graphene at liquid helium temperature are also highly desirable because scattering by phonons in this regime will be reduced, whereas the observables associated with many-body physics are expected to be enhanced. We anticipate that future studies will address yet another unresolved issue pertaining to the analysis of the linewidth of plasmonic modes in graphene that is determined by the ratio $\sigma'(\omega,q)/\sigma''(\omega,q)$. Plasmonic images, including those reported in (*2*–*4*), prompt us to reimagine the sheer scope of unresolved problems that can be tackled with this innovative experimental approach. ■

REFERENCES

1. D. N. Basov, R. D. Averitt, D. van der Marel, M. Dressel, K. Haule, *Rev. Mod. Phys.* **83**, 471 (2011).
2. M. B. Lundeberg *et al.*, *Science* **357**, 187 (2017).
3. D. N. Basov, M. M. Fogler, F. J. Garcia de Abajo, *Science* **354**, 195 (2016).
4. P. Alonso-González *et al.*, *Nat. Nano.* **12**, 31 (2017).
5. D. C. Elias *et al.*, *Nat. Phys.* **7**, 701 (2011).
6. J. González, F. Guinea, M. A. H. Vozmediano, *Phys. Rev. Lett.* **77**, 3589 (1996).
7. A. H. Castro Neto, F. Guinea, N. M. R. Peres, K. S. Novoselov, A. K. Geim, *Rev. Mod. Phys.* **81**, 109 (2009).
8. D. N. Basov, M. M. Fogler, A. Lanzara, F. Wang, Y. Zhang, *Rev. Mod. Phys.* **86**, 959 (2014).
9. C. F. Hirjibehedin, A. Pinczuk, B. S. Dennis, L. N. Pfeiffer, K. W. West, *Phys. Rev. B* **65**, 161309 (2002).
10. R. Krishna Kumar *et al.*, arXiv:1703.06672v1 (2017).
11. Z. Sun, D. N. Basov, M. M. Fogler, *Phys. Rev. Lett.* **117**, 076805 (2016).
12. A. S. McLeod *et al.*, *Nat. Phys.* **13**, 80 (2017).

10.1126/science.aan5361

BIOCHEMISTRY

How do miniproteins fold?

A high-throughput study yields libraries of miniproteins that help to explain how proteins are stabilized

By **Derek N. Woolfson,[1,2,3] Emily G. Baker,[1] Gail J. Bartlett[1]**

How does the amino acid sequence of a protein chain determine and maintain its three-dimensional folded state? Answering this question—a key aspect of the protein-folding problem (*1*)—would help to explain how multiple noncovalent interactions conspire to assemble and stabilize complicated biomolecular structures; to predict protein structure and function from sequence for proteins that cannot be characterized experimentally; and to design new protein structures that do not exist in nature (*2*). On page 168 of this issue, Rocklin *et al.* use parallel protein design on a massive scale to create thousands of miniprotein variants and to determine what sequences specify and stabilize these structures (*3*). The work opens up considerable possibilities for protein folding and design.

Miniproteins are polypeptides shorter than 40 to 50 residues with stable tertiary structures (folds) that contain a limited number of secondary structure elements, such as α helices and β strands. By contrast, larger proteins have hundreds of amino acids that are often arranged in complex three-dimensional structures. Thus, miniproteins simplify the protein-folding problem and potentially allow in-depth examinations of sequence-structure-stability relationships without complications from larger protein contexts. Unfortunately, only a few miniproteins that are stable without covalent cross-links or stabilizing metal ions are currently available for such studies (*4*).

In their study, Rocklin *et al.* combine high-throughput DNA synthesis and cloning (*5*, *6*) with methods for selecting stably folded proteins (*7*–*9*). They implement the latter by expressing libraries of miniproteins on the surface of yeast; tagging the displayed proteins with a fluorescent dye; and discriminating between stable and unstable folds through their ability to resist or succumb to protease treatment, respectively (see the figure). Proteins that survive are rescued by fluorescence-activated cell sorting and then identified by deep sequencing. However, the team's experiments go beyond a yes/no measure of protein resilience, providing a semiquantitative measure of stability.

To demonstrate the approach, the authors first apply their method to many variants of a small number of known miniproteins. With the method established, they turn their attention to four classes of de novo miniproteins, which they design computationally using Rosetta (*10*): ααα, βαββ, αββα, and ββαββ folds, where each Greek letter represents an α helix or a β strand in the peptide string.

"...Rocklin* et al. *have taken high-throughput, data-driven protein design, selection, and optimization to new heights..."

To cover swaths of sequence space, the team generate diverse libraries with minimal sequence identity between members.

They then use iterative rounds of protease selection and stability scoring, testing different hypotheses, and introducing tweaks to the design methods and protocols at each stage. The value of these tweaks is apparent from the improved success rate—the proportion of stable proteins in the starting library—which reaches 87% for one target. However, both the initial and final design success rates depend critically on the fold being targeted, with the ααα fold proving easiest and the αββα fold most difficult to optimize.

Through sequence analyses of many thousands of these new and also existing miniprotein folds from other studies, the authors highlight several key sequence and structural features. First, a long-established basic tenet of protein folding and design shines through: the importance of burying nonpolar surfaces. This is not surprising, but Rocklin *et al.* quantify the effect, showing that stable variants require more than 30 Å^2 for each residue of buried hydrocarbon.

Second, of the initial computational designs, those containing peptide fragments geometrically similar to ones known from the

[1]*School of Chemistry, University of Bristol, Cantock's Close, Bristol BS8 1TS, UK.* [2]*School of Biochemistry, University of Bristol, Medical Sciences Building, University Walk, Bristol BS8 1TD, UK.* [3]*Bristol BioDesign Institute, University of Bristol, Life Sciences Building, Tyndall Avenue, Bristol BS8 1TQ, UK. Email: d.n.woolfson@bristol.ac.uk*

Plasmonic imaging is gaining momentum

D. N. Basov and M. M. Fogler

Science **357** (6347), 132-133.
DOI: 10.1126/science.aan5361